J. Microbiol. Biotechnol. (2019), 29(1), 105–113
https://doi.org/10.4014/jmb.1712.12026

jmb

Zinc Ions Affect Siderophore Production by Fungi Isolated from the *Panax ginseng* Rhizosphere

Khalid Abdallah Hussein[1,2] and Jin Ho Joo[2]*

[1]*Botany and Microbiology Department, Faculty of Science, Assiut University, 71516, Assiut, Egypt*
[2]*Department of Biological Environment, Kangwon National University, Chuncheon 24341 , Republic of Korea*

Received: December 11, 2017
Revised: October 8, 2018
Accepted: October 9, 2018

First published online
October 10, 2018

**Corresponding author*
Phone: +82-33-250-6448;
Fax: +82-33-241-6640;
E-mail: jhjoo@kangwon.ac.kr

pISSN 1017-7825, eISSN 1738-8872

Although siderophore compounds are mainly biosynthesized as a response to iron deficiency in the environment, they also bind with other metals. A few studies have been conducted on the impact of heavy metals on the siderophore-mediated iron uptake by microbiome. Here, we investigated siderophore production by a variety of rhizosphere fungi under different concentrations of Zn^{2+} ion. These strains were specifically isolated from the rhizosphere of *Panax ginseng* (Korean ginseng). The siderophore production of isolated fungi was investigated with chrome azurol S (CAS) assay liquid media amended with different concentrations of Zn^{2+} (50 to 250 μg/ml). The percentage of siderophore units was quantified using the ultra-violet (UV) irradiation method. The results indicated that high concentrations of Zn^{2+} ion increase the production of siderophore in iron-limited cultures. Maximum siderophore production by the fungal strains was detected at Zn^{2+} ion concentration of 150 μg/ml except for *Mortierella* sp., which had the highest siderophore production at 200 μg/ml. One potent siderophore-producing strain (*Penicillium* sp. JJHO) was strongly influenced by the presence of Zn^{2+} ions and showed high identity to *P. commune* (100% using 18S-rRNA sequencing). The purified siderophores of the *Penicillium* sp. JJHO strain were chemically identified using UV, Fourier-transform infrared spectroscopy (FTIR), and matrix-assisted laser desorption/ionization time-of-flight mass spectrometer (MALDI-TOF-MS) spectra.

Keywords: Root-associated fungi, siderophore, Zn^{2+}, *Penicillium commune*

Introduction

Iron is one of the most common elements of the Earths' crust. It is available in the soil, with rare exceptions, as oxide hydrates, which have few dissociation constants [1]. In recent years, the production of siderophores by fluorescent pseudomonads in the rhizosphere has received great attention, due to their prospective role in the promotion of plant growth and bio-control of soil-borne diseases [2]. Most fungi produce siderophores [1], with few exceptions (*e.g.*, *Saccharomyces* species); nevertheless, *Saccharomyces cerevisiae* uses exotic siderophores [3]. Fungi produce a variety of siderophores, mainly hydroxamate. Biosynthesis expression and the uptake systems of siderophores are regulated by internal iron concentrations. However, siderophores form complexes with metals other than iron, such as actinides [4]. Dimkpa et al. [5] found that Al, Cd, Ni, and Cu stimulate the production of three different hydroxamate siderophores; namely, desferrioxamine B, desferrioxamine E, and coelichelin by *Streptomyces* sp. Tripathi *et al*. [6] stated that the inoculation of *Phaseolus vulgaris* with a Cd- and Pb-resistant and siderophore-producing strain of *Pseudomonas putida* KNPP enhanced plant growth, with cadmium and lead having no side effects on plant quality compared to the control. Various studies have assessed the concentration of Fe^{2+} and other heavy metal ions on siderophore-mediated iron uptake by microorganisms [5]. However, only a few studies have assessed the effect of Zn^{2+} ion concentrations on iron uptake. High concentrations of Zn^{2+} are toxic, inhibiting the aerobic respiratory chain [7]. Metal-resistant siderophore-producing microorganisms play a distinctive role in the

survival and promotion of plant growth in contaminated soils, by decreasing metal toxicity and providing plants with iron and other nutrients. Because of rapid industrial development, there is growing public concern over the potential accumulation of heavy metals in soils. The Zn content of farmland soils is frequently higher than that of natural soils. This phenomenon is mainly due to the application of commercial fertilizers, manure, and/or liming materials [8]. In addition, pesticides and fungicides containing Zn contribute to its presence in agricultural soils, where the element sometimes accumulates to reach values considerably higher than its optimum concentration as a nutrient, and it may be toxic to soil organisms [9]. The primary function of siderophores is to chelate Fe(III). They also form complex compounds with other heavy metals, such as Cd(II), Cu(II), and Zn(II) [10]. The ability to form complexes depends on the functionality of ligands, with several studies focusing on how siderophores impact the mobility of these metals in the environment [11, 12]. Thus, siderophores represent a valuable and environmentally friendly tool for removing metals from the soil. The present study investigated how Zn^{2+} influences siderophore production by a variety of rhizosphere fungal strains. In addition, the siderophores of a strong siderophore-producing strain were purified, identified, and characterized before possible siderophorogenic application to promote plant growth.

Materials and Methods

Micro-Organisms and Culture Conditions

Soil samples were collected from the rhizosphere of ginseng (*Panax ginseng*), which is an important economic herb cultivated and used mostly in Asia. The medicinal and commercial value of ginseng was discovered over ten centuries ago. Samples were collected in zipper bags and stored at 4°C. Twenty-three fungal strains belonging to different classes were isolated using the dilution plate technique and purified on Czapek's Agar medium containing 3% saccharose, 0.2% sodium nitrate, 0/1% dipotassium phosphate, 0.05% magnesium sulfate, 0.05% potassium chloride, 0.001% ferrous sulfate, and 1.5% agar. Stock cultures of fungi were preserved on 2% malt extract agar (MEA) slants grown at 27°C, and stored at 4°C before screening for siderophores.

Qualitative Chrome Azurol S (CAS) Assay for Siderophore Production

The fungal strains were sub-cultured on MEA slant tubes and incubated at 27°C. Five days later, the culture spores were scraped aseptically into sterile distilled water containing 0.1% Tween 80 and were homogenized with a vortex. A cell counting Neubauer chamber (Merck, Spain) was used. The spore concentration was adjusted to 1.0×10^6 conidia/ml. 10 ml of iron-free Czapek Dox Broth (pH 7.3), and then inoculated with 1 ml of the spore suspension. The cultures were incubated in shakers at 150 ×*g* and 27°C for 7 days. CAS-agar (100 ml) was prepared according to Schwyn and Neilands [13]. A 7.5 ml volume of 2 mM Chrome Azurol S was mixed with 1.5 ml iron solution (1 mM $FeCl_3.6H_2O$, 10 mM HCl). While stirring, 6.0 ml of 10 mM hexadecyl trimethyl ammonium bromide (HDTAB) solution was added, and the resulting blue solution was kept at 50°C. In addition, buffer solution was prepared using 0.6 gm of PIPES (piperazine-N,N′-bis [2-ethanesulfonic acid]) dissolved in 85 mL deionized water, and then adjusted to a final pH of 6.7 using 6M KOH. To this solution, 1.5 g agar was added and dissolved by heating it at 50°C. The blue and agar solutions were finally mixed. The Petri dishes (9 cm diameter) were prepared with 20 ml CAS-agar. After gelling, 5-mm diameter holes were made and dried for 2 h at 31°C. Each hole was filled with 100 µl culture supernatant. A non-inoculated media was used as the negative control, and the cell-free supernatants from fungal cultures were tested [14]. Plates were left overnight at 4°C, of which only the seven most clear positive strains were used in the subsequent analyses (Fig. 1).

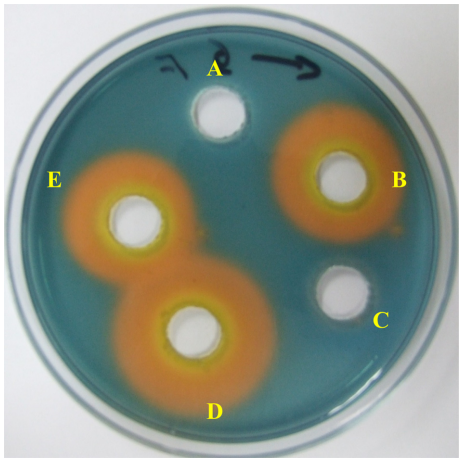

Fig. 1. CAS-agar diffusion (CASAD) assay to determine the most clear positive strains were used in the subsequent analyses.
(**A**) Control (non-inoculated medium). (**B**) *Penicillium commune* JJHO. (**C**) *Saccharomyces cerevisiae* K2S2 (negative fungal strain). (**D**) *Metarhizium anisopliae* KHAU. (**E**) *Trichoderma harzianum* TR274.

Effect of Zinc Ions on Siderophore Production

The fungal isolates were tested against different concentrations of Zn^{2+} ions, ranging between 50 and 250 µg/ml using $ZnSO_4$ in Czapek Dox Broth media (pH 7.3). Rhizobacteria strain *Pseudomonas aeruginosa* was selected from our previous study [15], and was stressed under the same concentrations of Zn^{2+} ions in Tris minimal media (pH 6.8). The pH was adjusted to 6.8 with 0.1 M

PIPES. The cultures were agitated to a stationary phase in the deferrated media. A 0.5-ml CAS test solution was added to 0.5 ml culture supernatant and 10 µl shuttle solution (0.2 M 5-sulfosalicylic acid) and was mixed thoroughly. The mixture was left for 5 min. The color development was assessed by absorbance (A_{630}) for the loss of blue color. A sterile culture medium was used as a blank, while the non-inoculated medium, CAS, and shuttle solutions were used as references. The siderophore units were evaluated by the following principle:

$$[(Ar\text{-}As)/Ar] \times 100 = \%\ \text{siderophore units}$$

where (Ar) is the absorbance value of the reference, and (As) is the absorbance value of the sample. The investigation was conducted in three replicates. The average of the three replicates was used for all analyses.

Identification of Strains

The fungi strains were identified provisionally by direct microscopic examination and culture characteristics according to Qi [16], Kong [17], and Zhang [18]. To a 1.5-ml Eppendorf tube containing 500 ml lysis buffer (400 mM Tris-HCl [pH 8.0], 60 mM ethylene diaminetetra acetic acid [EDTA] [pH 8.0], 150 mM NaCl, 1% sodium dodecyl sulfate), and a small lump of mycelia from young cultures were added with a sterile toothpick. The toothpick was also used to disrupt the lump of mycelia. The tube was left at room temperature for 10 min. After adding 150 ml potassium acetate (pH 4.8; which was made from 60 ml of 5 M potassium acetate, 11.5 ml glacial acetic acid, and 28.5 ml distilled water), the tube was briefly vortexed and spun at 10,000 ×*g* for 1 min. The supernatant was transferred to another 1.5-ml Eppendorf tube and centrifuged again. After transferring the supernatant to a new 1.5-ml Eppendorf tube, an equal volume of isopropyl alcohol was added. The tube was mixed by gentle inversion, spun at 10,000 ×*g* for 2 min, and the supernatant was discarded. The resulting pellet of DNA was washed in 300 ml of 70% ethanol. Then, the pellet was spun at 10,000 ×*g* for 1 min, and the supernatant was discarded. The air-dried DNA pellet was dissolved in 50 ml of deionized H_2O, and 1 ml of the purified DNA was used in 25 to 50 ml of PCR mixture. The extractions were completed in duplicate for each sample. The universal primers used for fungal amplification were ITS1: 5′ TCC GTA GGT GAA CCT GCG G 3′ and ITS4: 5′-TCCTCCGCTTATTGATATGC-3′ [19]. PCR amplification was performed in a thermal cycler for 30 cycles using denaturation of DNA at 94ºC for 1 min, primer annealing at 56ºC for 30 sec, and primer extension at 72ºC for 1 min. The PCR product was sequenced at Macrogen Inc. To identify the isolated fungi, the partial gene sequence was matched with the full sequence presented in the GenBank database via the BLAST search (NCBI). The fungal 18S rRNA gene fragments were aligned using Clustral W [20]. Sequence alignment and phylogenetic analysis with homologous genes were performed using DNAstar software (version 5.01).

Extraction and Purification

The culture was centrifuged and the pH of the supernatant was decreased to pH 2.0 by 12 M HCl and was then extracted with 0.4 volume of ethyl acetate. The fractions of ethyl acetate were collected and concentrated by rotary vacuum evaporation. The concentrated dried fractions were dissolved in deionized H_2O before column purification. Fifty grams of Sephadex LH-20 was suspended in methanol with shaking for about 30 min. The suspension was poured into a glass column of 50 × 1.5 cm diameter and equilibrated by four-bed volumes of methanol. The sample was concentrated and loaded onto the column and eluted by methanol that was four-bed volumes of the column. Separated fractions were placed in 100-ml flasks to test the extracted siderophores using aluminum-backed TLC plates coated with a 0.25-mm layer of silica gel using solvent system acetic acid:water:butanol (3:5:12, v/v). Iron-binding compounds were identified by spraying the TLC plates with CAS assay reagent. Autoclave-sterilized filter paper discs (10-mm diameter) were also impregnated with Sephadex LH-20 purified siderophore solution (15 µl). The discs were placed using sterile forceps on CAS-Agar plate. Color development around the discs was determined after incubation overnight at 4°C. Positive fractions were collected together and dried by rotary vacuum evaporator, and were then lyophilized and stored at −20°C. The Csáky and Arnow [21, 22] assays were also performed to differentiate between catechol- and hydroxamate-type siderophore.

Spectra Analysis Instruments

Matrix-Assisted Laser Desorption/Ionization Time-of-Flight Mass Spectrometer (MALDI-TOF-MS) analysis was performed by adopting positive ion mode on a time-of-flight mass spectrometer (Bremen, Daltonics Bruker, Microflex), with a 1.25-m flight tube. Desorption/ionization was acquired by using a 337-nm nitrogen laser with a 3-ns pulse width. Available acceleration potential was +20 kV on average. The spectra included in this paper represent a range of 100–200 laser shots. Laser power was fixed to be slightly beyond the threshold to obtain a good determination and signal-to-noise ratios. The analysis was repeated at least three times to check reproducibility. The absorption spectra of the constituents were detected using a UV–vis spectrometer (Perkin Elmer) from 300–700 nm. Transmission infrared spectra were obtained via KBr plates (4,000–400 cm^{-1}) on 8300 FT-IR spectrophotometers.

Statistical Analysis

All results were statistically analyzed using the SAS package (ver. 9.1). Means of three replicates were subjected to one-way ANOVA [23].

Results

Siderophore-Producing Strains

A total of 23 isolates were selected at random based on

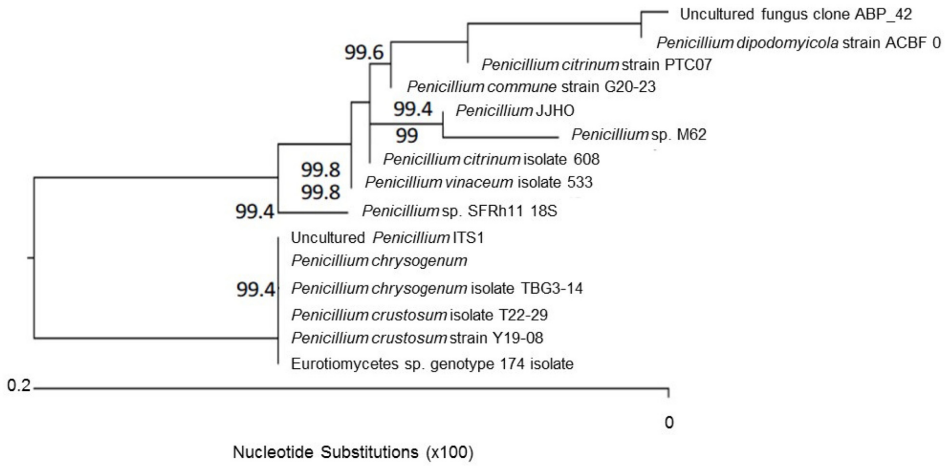

Fig. 2. Phylogenetic tree designed by neighbor-closing analysis of 18S rRNA gene sequence to show the position of *Penicillium* JJHO, the siderophore-producer isolate among the genus *Penicillium*.

P. commune (GU723445), *P. chrysogenum* (JX139710), *P. crustosum* (HQ262518), *P. dipodomyicola* (GQ161752), *Eurotiomycetes* sp (JQ761933), *P. citrinum* (JN206678), *P. chrysogenum* (JF731274), *Penicillium* sp. (HQ443258), Uncultured *Penicillium* (FN394532), Uncultured fungus clone ABP_42 (JF497145), *Penicillium* sp. (HM573339), *P. crustosum* (GU134895), *P. vinaceum* (DQ681340), *P. citrinum* (DQ681331), *P. rubens* (JX003126), *Eupenicillium crustaceum* (AB479321).

differences in the morphological features of the colonies for further study. The strongest siderophore-producing strain, *Penicillium* sp. JJHO, was subjected to siderophore purification. *Penicillium* sp. JJHO had a high identity (99% using 18S-rRNA sequencing) to *P. commune*. It was characterized by slow growth on MEA, with a grey-green colony and blue conidia. The 18S rRNA analysis showed that the isolate of *Penicillium* sp. JJHO had 100% nucleotide base homology with *P. commune*. The structure of the phylogenetic tree was produced by the online tool PhyML (www.phylogeny.fr), and visualization of the tree was achieved using TreeDyn. The ribosomal RNA sequence of *Penicillium* sp. JJHO was saved in the NCBI GeneBank under the accession number KC549672. Details of the phylogenetic affiliation of the representative sequence for *Penicillium* sp. JJHO strain are shown in (Fig. 2).

Effect of Zn Ions on Siderophore Production

The effect of Zn^{2+} on the siderophores of the studied microbial strains was quantified using a universal CAS assay [14]. Supernatants containing the siderophores of each sample were identified by a typical pinkish-red color. Zn^{2+} ions influenced the production of the siderophores of all of the studied microbial strains. The optimum siderophore production by the fungal strains was detected at a Zn^{2+} ion concentration of 150 μg/ml, except for *Mortierella* sp., which had the highest siderophore production of 39.62% of units at 200 μg/ml. *Penicillium* sp. JJHO and *Metarhizium anisopliae* had the highest siderophore production, producing 72.65 and 72.43% of units, respectively. *Rhodosporidium toruloides* and *Trichoderma* sp. were the most strongly influenced by the presence of the Zn^{2+} ions in the defferated media. The former produced 13.76 and 18.52% of the units in the control and at 50 μg/ml Zn^{2+} ion, respectively, while *Trichoderma* sp. produced 33.11 and 63.73% of the units, in the control and at 50 μg/ml Zn^{2+} ion, respectively. *Fusarium oxysporum* had almost the same siderophore production at 150 and 200 ug/ml concentration of Zn^{2+} ions, producing 68.76 and 68.62% of units, respectively. At a 250 μg/ml concentration of Zn^{2+} ions, the two fungal strains (*Rhodosporidium toruloides* and *Mortierella turficola*) had the lowest siderophore production compared to the control. Otherwise, the siderophore production of most of the fungal isolates was significantly higher than that of the control (Table 1). *Trichoderma* sp. produced 18.52% of the siderophore units in the control and 63.39% of siderophore units in the 250 μg/ml Zn^{2+} treatment. However, the bacterial specimen *Pseudomonas aeruginosa* produced 36.9% of the units in the control and 25.05% of the units in the 250 μg/ml Zn^{2+} treatment (lower than the control). The bacterium *P. aeruginosa* only had the highest siderophore production at 100 μg/ml Zn^{2+} concentration, whereas the fungal strain *Trichoderma* sp. had the highest production at 150 μg/ml Zn^{2+} ion concentration.

Table 1. Zn^{2+} effect on siderophore synthesis by several fungal species.

Fungal Strain	Class	Zn^{2+} Concentration					
		0 μg ml^{-1}	50 μg ml^{-1}	100 μg ml^{-1}	150 μg ml^{-1}	200 μg ml^{-1}	250 μg ml^{-1}
Aspergillus versicolor Mir	Ascomycetes	55.35 ± 0.20	48.19 ± 0.13	58.76 ± 0.20	59.54 ± 0.40	53.06 ± 0.26	50.91 ± 0.40
Penicillium commune JJHO	Ascomycetes	67.37 ± 0.26	69.42 ± 0.33	69.46 ± 0.26	72.65 ± 0.27	70.95 ± 0.27	69.42 ± 0.15
Mortierella turficola CQ1	Zygomycetes	32.19 ± 0.20	33.55 ± 0.26	31.06 ± 0.39	37.96 ± 0.33	39.62 ± 0.33	34.46 ± 0.23
Fusarium oxysporum FCHA	Ascomycetes	46.65 ± 2.16	66.93 ± 0.46	67.36 ± 0.26	68.76 ± 0.53	68.62 ± 0.77	66.15 ± 0.77
Metarhizium anisopliae KHAU	Ascomycetes	68.63 ± 0.46	69.02 ± 0.38	71.25 ± 0.20	72.43 ± 0.40	71.86 ± 0.50	58.71 ± 0.52
Rhodosporidium toruloides K-1-8	Basidiomycota	13.76 ± 0.39	33.11 ± 0.15	33.21 ± 0.15	34.82 ± 0.27	31.45 ± 0.69	22.49 ± 0.46
Trichoderma harzianum TR274	Ascomycetes	18.52 ± 0.72	63.73 ± 0.30	66.01 ± 0.59	67.63 ± 0.60	65.27 ± 0.47	63.39 ± 0.33

Means with the same letter within a row are not significantly different at $p < 0.05$.

Extraction and Spectra Analysis of *Penicillium* sp. JJHO Siderophores

The siderophores of *Penicillium* sp. JJHO strain were only positive to the Csalky test. However, *Pseudomonas aeruginosa*, a rhizobacterial example, showed a positive reaction to Arnow's assay. These results confirm the presence of hydroxamate siderophores and catecholate types in these two strains, respectively. The highest siderophore production of fungi was shown by *Penicillium* sp. JJHO, which produced 72.65% of units. Ten fractions were obtained through a chromatography separation column by Sephadex LH-20. An impregnated filter paper disc from each fraction was

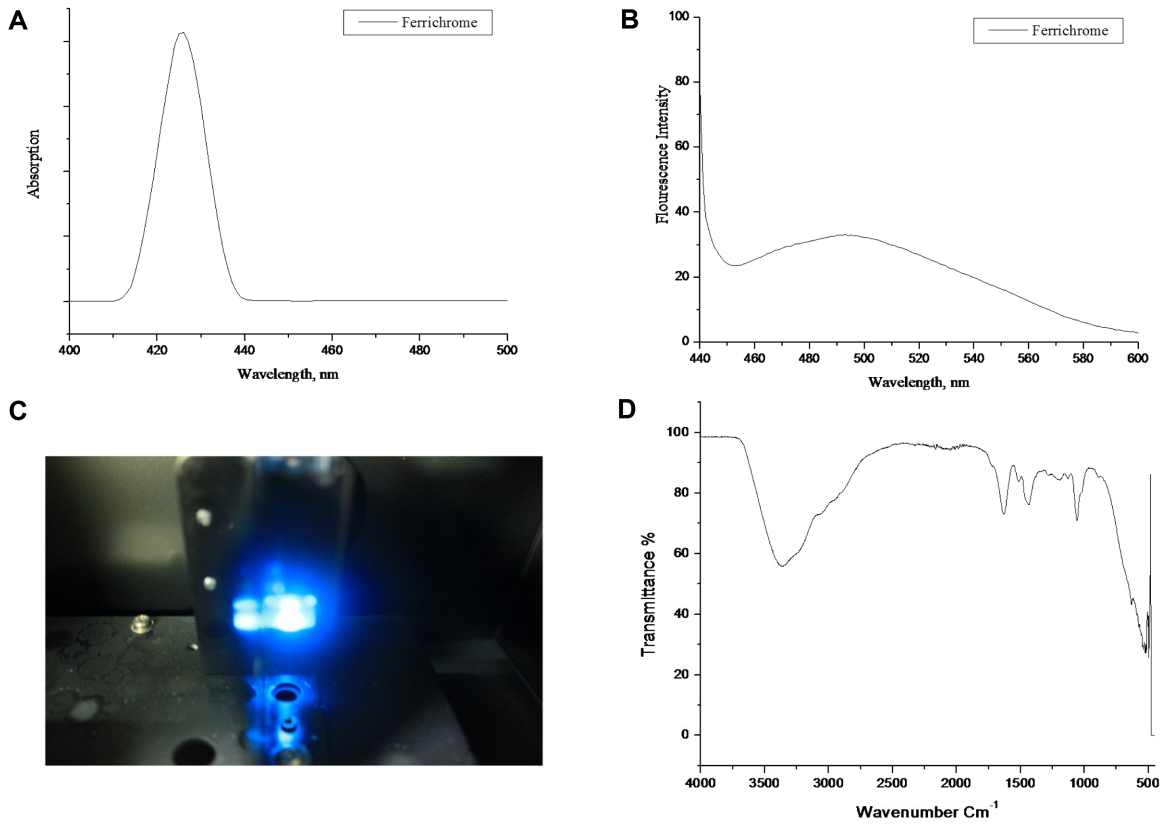

Fig. 3. Characterization of ferrichrome using spectroscopic techniques.

(**A**) UV absorption spectroscopy. (**B**) Fluorescence emission at excitation 425 nm. (**C**) Photographic emission of ferrichrome at wavelength of 425 nm showing blue color. (**D**) Shows the FTIR spectra of ferrichrome.

Table 2. FT-IR of the function groups in ferrichrome.

Classes	Function groups	Bands cm^{-1}
Amines	N-H stretch (1 per N-H bond)	3400
	N-H bend	1500
	C-N Stretch (alkyl)	1200
	N-H bend (oop)	~800
Amides	N-H stretch	3500
	C=O stretch	1680-1630
	N-H bend	1640-1550
Carboxylic acids	O-H stretch	3400
	C=O stretch	1700
	C-O stretch	1210

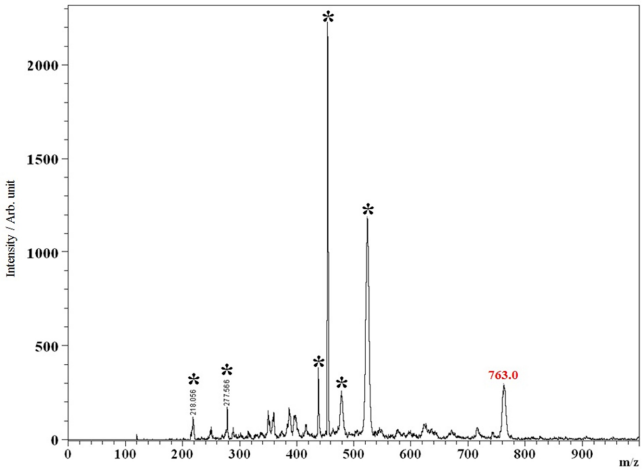

Fig. 4. MALDI-TOF-MS spectra of ferrichrome in positive mode.
(*) indicates peaks corresponding to the matrix ions.

placed on the CAS Agar plate. Only the fractions that turned the blue CAS Agar to a clear orange or yellow color were used. Using acetic acid:water:butanol (3:5:12, v/v) as the mobile phase, iron-binding compounds were confirmed by spraying the TLC plates with CAS assay solution. UV spectra of the Sephadex LH-20 purified fungal siderophores showed that absorption peaked at 425 nm (Figs. 3A and 3B). Ferrichrome at the excitation wavelength (425 nm) showed blue fluorescence (Fig. 3C). FT-IR spectra (Fourier Transform Infrared Spectroscopy) of the compound indicated the presence of an amide (NH-C=O), which is the main functional group in the compound. The compound was investigated from the peaks at wavelengths of 1,640, 1,680, 3,500 cm^{-1} and was assigned as N-H bending, C=O stretching, and N-H stretching, respectively (Table 2). The chelation or coordination of the compound with Fe (III) occurred via the acidic bond of the nitroso group N-O, which was investigated at 1,490 cm^{-1} and 1,150 cm^{-1}, and was assigned as an asymmetric stretch (strong) and a symmetric stretch (strong), respectively (Fig. 3D). Ferrichrome has a molecular formula of $C_{27}H_{42}N_9O_{12}$, producing a molecular weight of 740.52 g/mol. Based on the detected MALDI spectra, the molecular weight peaked at 763.0 Da as $[Ferrichrome+Na]^+$ (Fig. 4).

Discussion

Microorganisms with the most effective siderophore-mediated iron uptake have a competitive advantage and are of use for biocontrol and as biofertilizers. Heavy metals have an extreme effect on siderophore production. The presence of Co, Cd, and Zn in the media improved the production of siderophores, whereas Mn and Mo decreased production [5]. Specific nutrients are required for siderophore secretion, and might vary from one microorganism to another; however, iron-controlled conditions stay unchanged, contributing an energetic role in its secretion [24].

This study demonstrated the impact of Zn^{2+} ion concentrations on siderophore production by a variety of fungi. Optimum siderophore production by the fungal strains was attained at Zn^{2+} ion concentrations of 150 μg/ml, except for *Mortierella* sp., which had the highest siderophore production of 39.62% units at 200 μg/ml. Our previous studies showed that *P. aeruginosa* is one of the most important PGPR strains, producing 76.53% of siderophore units [15]. *Trichoderma harizianum* is a key PGPF and biocontrol agent, exhibiting high siderophore production [25]. In the current study, *Trichoderma* sp. TR274, as well as a bacterial specimen, showed the strong effect of Zn ions on the induction of siderophores. Thus, in contrast to a bacterial strain, fungal strains showed higher siderophore production at a 250 μg/ml concentration of Zn^{2+} (Fig. 5). There are two possible explanations for the motivating impact of heavy metals on siderophore biosynthesis. First, heavy metals might be required in the siderophore biosynthesis pathway or their control [26]. Second, the amount of free siderophores might decline when complexes are formed with heavy metals ions. Thus, soluble iron concentration is also diminished. As iron does not stimulate the generation of siderophores, more siderophore molecules would then be delivered [5].

The biochemical pathway of ferrichrome synthesis is poorly understood. At concentrations of 250 μg/ml Zn^{2+} ions, only two fungal isolates showed lower and significant

siderophore production than the control. *Trichoderma* sp. produced 18.52% of siderophore units in the control and 63.39% of siderophore units in the 250 µg/ml Zn^{2+} treatment. Moreover, *P. aeruginosa* produced 36.95% of units in the control and 25.05% of units in the 250 µg/ml Zn^{2+} treatment.

Zn^{2+} is of great importance for microorganisms and is a catalytic co-factor for many proteins, including Zn^{2+} finger DNA-binding proteins. Zn^{2+} is also an intracellular additional messenger in many signal transduction pathways [27]. Furthermore, superoxide dismutases (SODs) in fungi are essential for the detoxification of reactive oxygen species (ROS) generated by host cells, and are zinc-dependent enzymes [28]. Consequently, in iron, there is competition for Zn^{2+} ions [29]. Fungi secrete a variety of hydroxamate siderophores. The synthesis of ferrichrome has been characterized for one member of the Ascomycete and Basidiomycete classes [30]. This class of siderophore includes other compounds, such as ferrichrome, ferricrocin, ferrichrome A, ferrichrome B, and malonichrome [31].

Most ferrichrome siderophore compounds are cyclic hexapeptides that play vital functions in fungal biochemistry [31]. Ferricrocin promotes the germination of asexual spores of *Neurospora crassa* by storing iron reserves inside the spores [32]. This activity is similar to the role of ferrichrome-type in the asexual reproduction of *A. nidulans* [33] and *P. chrysogenum* [32]. The fungal siderophore structures are mostly hydroxamates, which are similar to bacterial siderophores [34]. Fungal hydroxamates have similar biosynthetic pathways because of their similar basic unit, Nd-acyl-Nd-hydroxy ornithine [35]. Frisvad and Larsen [36] found that *A. fumigatus* produces a peptide synthetase that is essential for ferrichrome production. Miethke and Marahiel [37] detected L-cis-ferrichrome in *P. parvum*, while Grundlinger *et al*. [35] detected it in *N. crassa*, *A. quadricinctus*; however, the authors were not able to recognize D-cis-ferrichrome.

The siderophores produced by organisms might be restricted to a particular structural family; however, in a few cases, the fungus biosynthesizes siderophores that belong to different structural families [4]. Taxonomic studies of Ustilaginales showed that *Tilletiaria*, *Graphiola*, *Protomyces*, and parasitic Ustilaginales form ferrichrome-type siderophores, whereas saprophytic Ustilaginales form rhodotorulic acid [27, 38]. The investigation of the fungal siderophores of *Penicillium* sp. JJHO using UV and fluorescence spectroscopy data in this study showed an absorption peak at a wavelength of 425 nm. Also, the compound at the excitation 425 nm wavelength showed

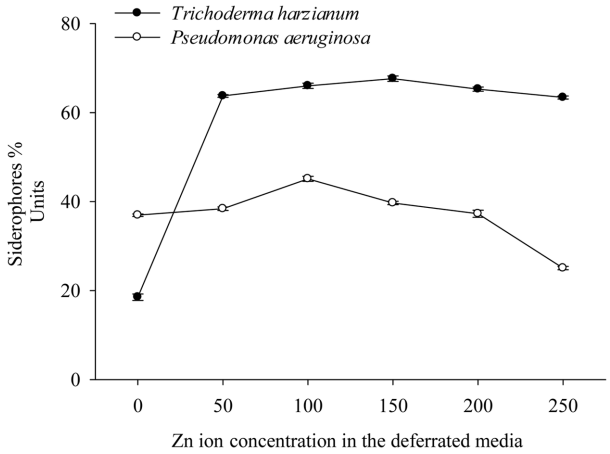

Fig. 5. Shows the optimal concentrations of Zn^{2+} ions in the deferrated media for siderophores generation by *Trichoderma harzianum* in contrast, and bacterial case.

blue fluorescence. These results suggest the presence of Ferrichrome. Masuda *et al*. [39] suggested that ferrichrome shows peak absorption at 425 nm. Ferrichrome was stirred at 25°C in a 1-ml cell, and the excitation wavelength (λ_{exc}) was set at 425 nm, with fluorescence emission (λ_{em}) being measured at 500 nm, confirming the results obtained by Hannauer *et al*. [40].

The FTIR of the compound extracted from *Penicillium* sp. JJHO showed that the compound displayed three peaks at wave numbers 1,640, 1,680, and 3,500 cm^{-1}, which were assigned as N-H stretching, C=O stretching, and, N-H bending, respectively. The chelation or coordination of the compound with Fe (III) occurs via the acidic bond of the nitroso group N-O. This group was investigated at 1,490 cm^{-1} and 1,150 cm^{-1}, which were assigned as an asymmetric stretch (strong) and symmetric stretch (strong), respectively. Ferrichrome is a cyclic hexapeptide made out of three glycines and three adjusted ornithine residues that unite Fe(III) with the hydroxamate groups [-N(OH)C(=O)C-].

Ferrichrome was initially isolated in 1952, and was observed to be delivered by the fungi genera *Aspergillus*, *Ustilago*, and *Penicillium* [41]. The main functional group in the compound is the amide (NH-C=O). The cellular siderophores of *A. nidulans* are ferricrocin and triacetylfusigen. However, *P. chrysogenum* contains ferrichrome. The conidia of both species (*A. nidulans* and *P. chrysogenum*) lack siderophores at high salt concentrations [42]. Kröber *et al*. [43] showed that *Trichophyton rubrum* produces the same siderophore ferrichrome C and ferricrocin, as well as *Microsporum gypseum*, *M. audouinii*, and *M. canis*. In

comparison, *T. tonsurans* and *T. mentagrophytes* only produce ferrichrome [42].

Filamentous ascomycete genomes mostly contain one or two nonribosomal peptide synthetases (NRPS). However, *Botrytis cinerea* might possess three ferrichrome synthetases of NRPS [44]. Bushley and Turgeon, 2010, characterized the subfamilies of fungal NRPSs. Their analyses suggested that mono/bimodular NRPSs have more early origins and more conserved domain architectures than most multi-modular NRPSs. Phylogenetic analyses of ferrichrome synthetases provided support for an ancestral duplication event, producing two main families. The authors also supported the hypothesis that siderophore synthetases are derived from a hexamodular ancestral gene, likely created by the tandem doubling of complete NRPS modules [45].

Correlations between the types and taxonomy of siderophores have been demonstrated in bacteria. However, there is a weak correlation between siderophore generation and taxonomic classification in fungi [4]. Our study showed that, based on the MALDI-TOF spectra of the fungal siderophores, the characteristics of ferrichrome (M.Wt 763.0 Da) can be assigned as $[Ferrichrome+Na]^+$. Ferrichrome has the molecular formula of $C_{27}H_{42}N_9O_{12}$, which gives a molecular weight of 740.52 g/mol.

Siderophores bind to other metals, in addition to binding strongly with Fe(III). Because of their metal-chelating ability, there might be potential applications for siderophores in medical and environment-associated problems [4]. Siderophore types are also being investigated for other applications, including the decorporation of actinides, as anticancer and antimicrobial agents, and for transporting drugs into microorganisms [4]. In conclusion, it is necessary to understand the chemistry and biology of siderophores before applying them or their analogs to the field of agriculture. Heavy metals affect the siderophore production of microbes. By analyzing the effect of Zn^{2+} on siderophore production in fungi, we showed that Zn^{2+} ions alone are able to activate siderophore synthesis in microbes. According to UV spectra, FTIR, and MALDI-TOF data, the investigated fungal siderophores produced by the *Penicillium* sp. JJHO strain are likely to be hydroxamate-type ferrichrome. Moreover, the presence of adequate quantities of heavy metals might promote plant growth.

Acknowledgment

This work was supported by the National Research Foundation of Korea (NRF) grant funded by the Korea government (Ministry of Science, ICT & Future Planning) (No.2017R1A2B1009738).

Conflict of Interest

The authors have no financial conflicts of interest to declare.

References

1. Pereg L, McMillan M. 2015. Scoping the potential uses of beneficial microorganisms for increasing productivity in cotton cropping systems *Soil. Biol. Biochem.* **80:** 349-358.
2. Neubauer U, Nowack B, Furrer G, Schulin R. 2000. Heavy metal sorption on clay minerals affected by the siderophore desferrioxamine B. *Environ. Sci. Technol.* **34:** 2749-2755.
3. Aznar A, Dellagi A. 2015. New insights into the role of siderophores as triggers of plant immunity: what can we learn from animals? *J. Exper. Bot.* **66:** 3001-3010.
4. Renshaw JC, Robson GD, Trinci APJ, Wiebe MG, Livens FR, Collison D, *et al*. 2002. Fungal siderophores structures, functions and applications. *Mycol. Res.* **106:** 1123-1142.
5. Dimkpa CO, Svatos A, Dabrowska P, Schmidt A, Boland W, Kothe E. 2008. Involvement of siderophores in the reduction of metal-induced inhibition of auxin synthesis in *Streptomyces* spp. *Chemosphere* **74:** 19-25.
6. Tripathi M, Munot HP, Shouche Y, Meyer JM, Goel R. 2005. Isolation and functional characterization of siderophore-producing lead- and cadmium-resistant *Pseudomonas putida* KNP9. *Curr. Microbiol.* **50:** 233-237.
7. Bazihizina TC, MartiL RA, Spinelli F, Giordano C, Caparrotta S, Gori M, Azzarello E, Mancuso S. 2014. Zn^{2+} induced changes at the root level account for the increased tolerance of acclimated tobacco plants. *J. Exp. Bot.* **65:** 4931-4942.
8. Kabir E, Ray S, Kim K, Yoon H, Jeon E, Kim Y, *et al*. 2012. Current status of trace metal pollution in soils affected by industrial activities. *Scientific World Journal* 916705.
9. Liu M, Lia Y, Zhanga W, Yaojing W. 2013. Assessment and Spatial distribution of zinc pollution in agricultural soils of Chaoyang, China. *Procedia Environ. Sci.* **18:** 283-289.
10. Johnstone TC, Nolan EM. 2015. Beyond iron: non-classical biological functions of bacterial siderophores. *Dalton Trans.* **14:** 6320-6339.
11. Saha M, Sarkar S, Sarkar B, Sharma BK, Bhattacharjee S, Tribedi P. 2016. Microbial siderophores and their potential applications: a review. *Environ. Sci. Pollut. Res. Int.* **23:** 3984-3999.
12. Ahmed E, Holmstrom SJM. 2014. Siderophores in environmental research: roles and applications: minireview. *Microb. Biotechnol.* **7:** 196-208.
13. Schwyn B, Neilands, J.B. 1987. Universal chemical assay for the detection and determination of siderophores. *Anal. Biochem.* **160:** 47-56.

14. Naidu AJ, Yadav M. 1997. Influence of iron, growth temperature and plasmids on siderophore production in *Aerornonas hydrophila*. *J. Med. Microbiol*. **47:** 833-838.
15. Hussein KA, Joo JH. 2017. Stimulation, purification, and chemical characterization of siderophores produced by the rhizospheric bacterial strain *Pseudomonas putida. Rhizosphere* **4:** 16-21.
16. Qi Z. 1997. Fungi of China: *Aspergillus* et *teleomorphi cognate*. pp. 76-82. (Vol.5) Science Press, Beijing, China,.
17. Kong H. 2007. Flora *Fungorum Sinicorum.* pp. 283. (Vol. 35): *Penicillium* et *teleomorphi cognati*. Science Press, Beijing.
18. Zhang Z. 2003. *Cladosporium*, *Fusicladium*, *Pyricularia*. Flora Fungorum Sinicorum. pp. 297. (Vol. 14) Science Press, Beijing, China.
19. Herlemann DP, Labrenz M, Jürgens K, Bertilsson S, Waniek JJ, Andersson AF. 2011. Transitions in bacterial communities along the 2000 km salinity gradient of the Baltic Sea. *ISME J.* **5:** 1571-1579.
20. Thompson J, Higgins D, Gibson T. 1994. Clustal W: improving the sensitivity of progressive multiple sequence alignment thr ough sequence weighting, positionspecific gap penalties and weight matrix choice. *Nucleic Acids Res.* **22:** 4673-4680.
21. Csáky TZ. 1948. On the estimation of bound hydroxylamines in biological materials. *Acta Chem. Scand.* **2:** 450-454.
22. Arnow LE. 1937. Colorimetric determination of the components of 3,4-dihydroxyphenylalanine tyrosine mixtures. *J. Biol. Chem.* **118:** 531-537.
23. SAS Institute Inc, SAS, SAS/STAT 9.1 User's Guide. 2004. SAS Institute Inc., Cary, NC, USA.
24. Ahmed E, Holmström SJM. 2014. Siderophores in environmental research: roles and applications *Microb. Biotechnol.* **7:** 196-208.
25. Hussein KA, Joo JH. 2012. Comparison between Siderophores Production by Fungi Isolated from Heavy Metals Polluted and Rhizosphere Soils. *Kor. J. Soil Sci. Fert.* **45:** 798-804.
26. Rajkumar M, Freitas H. 2009. Effects of inoculation of plantgrowth promoting bacteria on Ni uptake by Indian mustard. *Bioresour. Technol*. **99:** 3491-3498.
27. Yamasaki S, Sakata-Sogawa K, Hasegawa A. 2007. Zinc is a novel intracellular second messenger. *J. Cell Biol.* **177:** 637-645.
28. Huang J, Canadien V, Lam GY. 2009. Activation of antibacterial autophagy by NADPH oxidases. *Proc. Natl. Acad. Sci. USA* **106:** 6226-6231.
29. Corbin BD, Seeley EH, Raab A. Feldmann J, Miller MR, Torres VJ, Anderson KL, *et al*. 2008. Metal chelation and inhibition of bacterial growth in tissue abscesses. *Science* **15:** 962-965.
30. Schwecke T, Goettling, K, Durek P, Duenas I, Kaeufer NF, Zock ES, *et al*. 2006. Nonribosomal peptide synthesis in *Schizosaccharomyces pombe* and the architectures of ferrichrome-type siderophore synthetases in fungi. *Chem. Biochem.* **7:** 612-622.
31. Rossbach S, Wilson TL, Kukuk ML, Carty HA. 2000. Elevated zinc induces siderophore biosynthesis genes and a zntA-like gene in *Pseudomonas fluorescens. FEMS Microbiol. Lett.* **1:** 61-70.
32. Carroll CS, Nesbitt JR, Henry KA, Pinto LJ, Moinzadeh M, Scott JK, *et al.* 2012. Structural requirements for the activity of the MirB ferrisiderophore transporter of *Aspergillus fumigates* isabelle raymond-bouchard. *Eukaryot Cell*. **11:** 1333-1344.
33. Eisendle M, Oberegger H, Zadra I, Haas H. 2003. The siderophore system is essential for viability of *Aspergillus* nidulans: functionalanalysis of two genes encoding l-ornithine N 5-monooxygenase (sidA) and a non-ribosomal peptide synthetase (sidC). *Mol. Microbiol.* **49:** 359-375.
34. Plattner H, Diekmann H. 1994. Enzymology of siderophore biosynthesis. In Metal Ions in Fungi (G. Winkelmann & D. R. Winge, eds) pp. 99-116. Marcel Dekker, New York.
35. Gründlinger M, Yasmin S, Lechner BE, Geley S, Schrett M, Hynes M, *et al.* 2013. Fungal siderophore biosynthesis is partially localized in peroxisomes. *Mol. Microbiol.* **88:** 862-875.
36. Frisvad JC, Larsen TO. 2016 Extrolites of *Aspergillus fumigatus* and other pathogenic species in *Aspergillus* section fumigati. *Front. Microbiol.* **6:** 1485.
37. Miethke M, Marahiel MA. 2007. Siderophore-based iron acquisition and pathogen control. *Mol. Biol. Rev.* **71:** 3413-4511.
38. Weaver RS, Kirchman DL, David A. 2003. Hutchins Utilization of iron/organic ligand complexes by marine bacterioplankton aquatic microbial ecology. *Aquat. Microb. Ecol.* **31:** 227-239.
39. Masuda T, Hayashi J, Tamagaki S. 2000. C_3-symmetric ferrichrome-mimicking Fe^{3+}complexes containing the 1-hydroxypyrimidinone Fe^{3+} binding moieties based on α-cyclodextrin: helicities in solvent environments. *J. Chem. Soci. Perkin Trans.* **2:** 161-167.
40. Hannauer M, Barda Y, Mislin GA, Shanzer A, Schalk IJ. 2010. The ferrichrome uptake pathway in *Pseudomonas aeruginosa* involves an iron release mechanism with acylation of the siderophore and recycling of the modified desferrichrome. *J. Bacteriol.* **192:** 1212-1220.
41. Tedstone AA, Lewis DJ, Brien P. 2016. Synthesis, properties, and applications of transition metal-doped layered transition metal dichalcogenides. *Chem. Mater.* **28:** 1965-1974.
42. Dimkpa C. 2016. Microbial siderophores: production, detection and application in agriculture and environment. *Endocytobiosis Cell Res.* **27:** 7-16.
43. Kröber A, Scherlach K, Hortschansky P, Shelest E, Staib P, Kniemeyer O, *et al*. 2016. HapX mediates iron homeostasis in the pathogenic dermatophyte *Arthroderma benhamiae* but is dispensable for virulence. *PLoS One* **11:** e0150701.
44. Bushley KE, Ripolland DR, Turgeon B. 2008. Module evolution and substrate specificity of fungal nonribosomal peptide synthetases involved in siderophore biosynthesis. *BMC Evoly. Biol.* **8:** 328.
45. Bushley KE, Turgeon BG, 2010. Phylogenomics reveals subfamilies of fungal nonribosomal peptide synthetases and their evolutionary relationships. *BMC Evol. Biol.* **10:** 26.